HHS Public Access

Author manuscript

PM R. Author manuscript; available in PMC 2023 April 01.

Published in final edited form as:

PM R. 2022 April ; 14(4): 472–485. doi:10.1002/pmrj.12623.

Investigating whole-brain metabolite abnormalities in the chronic stages of moderate or severe traumatic brain injury

Joanne C. Lin, PhD[1],

Christina Mueller, MS[1],

Kelsey A. Campbell, MA[1],

Halle H. Thannickal, BS[2],

Altamish F. Daredia, BS[1],

Sulaiman Sheriff, BSc[3],

Andrew A. Maudsley, PhD[3],

Robert C. Brunner, MD[4],

Jarred W. Younger, PhD[1]

[1]Department of Psychology, University of Alabama at Birmingham, Birmingham, Alabama, USA

[2]Department of Biology, University of Michigan, Ann Arbor, Michigan, USA

[3]Department of Radiology, Miller School of Medicine, University of Miami, Miami, Florida, USA

[4]Department of Physical Medicine and Rehabilitation, University of Alabama at Birmingham, Birmingham, Alabama, USA

Abstract

Background: Evidence suggests that neurometabolic abnormalities can persist after traumatic brain injury (TBI) and drive clinical symptoms such as fatigue and cognitive disruption. Magnetic resonance spectroscopy has been used to investigate metabolite abnormalities following TBI, but few studies have obtained data beyond the subacute stage or over large brain regions.

Objective: To measure whole-brain metabolites in chronic stages of TBI.

Design: Observational study.

Setting: University.

Participants: Eleven men with a moderate or severe TBI more than 12 months prior and 10 age-matched healthy controls completed whole-brain spectroscopic imaging.

Main Measures: Ratios of N-acetylaspartate (NAA), choline (CHO), and myoinositol (MI) to creatine (CR) were measured in whole-brain gray and white matter as well as 64 brain regions of

Correspondence: Joanne C. Lin, School of Pharmacy, Faculty of Medical and Health Sciences, University of Auckland, New Zealand. joanne.lin@auckland.ac.nz.

Disclosure: None declared.

SUPPORTING INFORMATION

Additional supporting information may be found online in the Supporting Information section at the end of this article.

interest. Arterial spin labeling (ASL) data were also collected to investigate whether metabolite abnormalities were accompanied by differences in cerebral perfusion.

Results: There were no differences in metabolite ratios within whole-brain gray and white matter regions of interest (ROIs). Linear regression showed lower NAA/CR in the white matter of the left occipital lobe but higher NAA/CR in the gray matter of the left parietal lobe. Metabolite abnormalities were observed in several brain regions in the TBI group including the corpus callosum, putamen, and posterior cingulate. However, none of the findings survived correction for multiple comparison. There were no differences in cerebral blood flow between patients and controls.

Conclusion: Higher MI/CR may indicate ongoing gliosis, and it has been suggested that low CHO/CR at chronic time points may indicate cell death or lack of healthy turnover and repair. However, with the small sample size of this study, we caution against the overinterpretation of our results. None of the findings within ROIs survived correction for multiple comparison. Thus, they may be considered possible avenues for future research in this area.

INTRODUCTION

Traumatic brain injury (TBI) is a prevalent public health issue and a major contributor to disability. An estimated 3.2–5.3 million people are living with a TBI-related injury in the United States.[1–4] Long-term consequences following a moderate-to-severe injury that persist beyond the initial recovery phase can include changes in cognitive functioning, behavior, mood, and motor and sensory function.[1]

Although neural cell damage may arise from the initial impact during a TBI, additional injury can occur via subsequent physiological mechanisms. The biochemical cascade of neuroinflammatory events following a TBI involves mobilization of immune cells, activation of microglia, and release of cytokines and chemokines at the site of injury.[5–7] Although this response is initially beneficial for healing damaged tissue, inflammation may persist long after structural recovery has plateaued, disrupting endogenous repair processes.[8–13] Chronically activated microglia release proinflammatory factors that can drive many of the persistent clinical symptoms after a TBI, such as profound pain sensitivity, fatigue, cognitive disruption, and mood disturbance.[8] Therefore, tissue damage and altered neuronal and glial metabolism may be critical determinants of the long-term impact of TBI and a promising target for treatment and outcome assessment in some patients.

A potential method for assessing tissue damage and neuronal and glial metabolism following TBI is magnetic resonance spectroscopy (MRS). MRS has been used to investigate metabolic abnormalities in N-acetylaspartate (NAA), choline-containing compounds (CHO), and creatine (CR), which are considered markers for neuronal integrity, cell membrane turnover, and cellular energetics, respectively.[14] Studies have been heterogeneous with respect to the severity of TBI, length of time from injury, and location of MRS acquisition; however, they generally support the idea that neurometabolic abnormalities persist after a TBI. For example, a recent large meta-analysis showed that elevated CHO/CR and lower NAA/CR ratios are frequently detectable at the subacute stage of a moderate-to-severe TBI (at least 8 days past the date of injury).[15] There is growing interest in myo-inositol (MI), an

astroglial marker and osmolyte,[16] which has been shown to be elevated in both acute[17] and chronic[18] stages of TBI.

The majority of MRS studies in patients with moderate-to-severe TBI have relied on measurements within discrete regions of interest (ROIs). Given the potentially diffuse nature of underlying brain changes following TBI,[19,20] single voxel or even two-dimensional MRS techniques may miss important elements of long-term pathophysiological consequences of TBI. The only two studies that obtained spectroscopic data over large brain regions in this population were limited to participants in the subacute stage - approximately 1 month past the date of injury.[21,22] The lack of whole-brain MRS data beyond the 1-year period of expected recovery means that little is known about the spatial distribution of metabolite alterations that persist long term. Such information would be critical to explaining why a significant proportion of TBI survivors continue to report symptoms such as depression,[23,24] fatigue,[25–27] and pain[28–30] long after their injury.

There are few long-term, whole-brain MRS studies that have investigated metabolite distributions at >12 months post injury in patients with moderate/severe TBI. A study by Maudsley et al investigated a single patient with moderate TBI on five occasions between 7 weeks and 28 months following injury. Significantly increased CHO and reduced NAA were observed in white matter regions at all subacute and chronic time points, corroborating previous findings of persistent microglial activation, gliosis, and/or glial scar formation.[31] In contrast, a longitudinal study of pediatric patients with moderate/severe TBI found that elevations in CHO in lobar regions and the corpus callosum observed at 3 months post injury had normalized by the chronic time point (average 16 months post injury).[32] In another study of pediatric patients, all metabolite ratios in patients with moderate TBI had fully recovered at 1 year; however, in patients with severe TBI, only cortical gray matter regions full recovered, whereas NAA ratios in white matter and subcortical regions remained significantly reduced.[33] It should be kept in mind when comparing results across studies, that different post-processing approaches were used, for example, z-score image analysis (Maudsley et al[34]), voxel averaging (Babikian et al,[32] Holshouser et al[33]).

In this study, whole-brain MRS data were acquired in a group of men who had experienced a moderate or severe TBI more than 12 months before and who reported ongoing pain and/or fatigue. Another group of male control participants without a history of TBI were also recruited. Arterial spin labeling (ASL) data were also collected to investigate whether metabolite abnormalities were accompanied by differences in cerebral perfusion. This was a prospective study and recruitment was limited to male participants as men have been shown to be at greater risk of having TBI[35,36]; therefore, for the purposes of this small study, it was important to maintain sample homogeneity. We hypothesized that individuals with TBI would show elevated CHO and MI and lower NAA than the control group, correlated with the severity of their clinical symptoms.

MATERIALS AND METHODS

Participants

Sixteen male participants who had experienced a moderate or severe nonpenetrating TBI and 12 male control participants were invited to participate in this study. For participants who had experienced a TBI, the inclusion criteria were (1) age between 18 and 55 years; (2) a nonpenetrating, moderate or severe TBI within the past 12–24 months (as defined by one or more of the following: Glasgow Coma Scale <13, duration of altered mental state or loss of consciousness >30 minutes, or posttraumatic amnesia >24 hours[1]); and (3) average self-reported pain and/or fatigue rating ≥4 on an 11-point (0–11) scale. Control participants were also aged between 18 and 55 years, had no history of brain injury, including mild TBI/concussion, stroke, or brain tumor, and had average self-reported pain and fatigue ratings of ≤2 on an 11-point scale. Exclusion criteria for both groups included (1) any magnetic resonance imaging (MRI) contraindications, (2) current or recent substance use (within the past 6 months), (3) any neurodegenerative or inflammatory conditions, and (4) a score of ≥20 on the Patient Health Questionnaire-9. All study procedures were approved by the institutional review board.

Study protocol

On the day of the study, all participants gave written informed consent before undergoing any research procedures. Participants then completed study questionnaires followed by the MRI acquisition (approximately 45 minutes).

Symptom questionnaires

In order to assess the severity of symptoms associated with TBI, the Brief Pain Inventory,[37] the Fatigue Severity Scale,[38] and the Hospital Anxiety and Depression Scale (HADS)[39] were administered. The pain intensity subscale of the Brief Pain Inventory was used as a measure of severity. The pain intensity score was calculated by taking a mean of four items (average, least, and worst pain over the last 24 hours, as well as present pain), scored on an 11-point (0–10) numerical rating scale. Pain interference measured how much pain interefered with daily activities and was calculated by taking a mean of seven items (relations with others, enjoyment of life, mood, sleep, walking, general activity, and working), scored on an 11-point (0–10) numerical rating scale. The Fatigue Severity Scale consists of nine questions and uses a seven-point (1–7) Likert scale (ranging from “strongly disagrees” to “strongly agrees”) and is designed to assess the connection between fatigue intensity and functional disability. The HADS is divided into an Anxiety subscale (HADS-A) and a Depression subscale (HADS-D), both containing seven items on a four-point (0–3) scale, and was used to measure states of anxiety and depression.

Image acquisition

Data were collected using a 3.0T Siemens Magnetom Prisma System with a 20-channel head/neck coil. A T1-weighted image was acquired for segmentation and anatomical reference using a magnetization prepared rapid gradient echo sequence: repetition time (TR) = 2000 msec; echo time (TE) = 2.51 msec; flip angle = 8°; 208 slices; slice thickness

= 0.9 mm; field of view (FOV) = 230 × 230 mm; matrix = 256 × 256; acquisition time (TA) = 5 min; voxel resolution = 0.9 × 0.9 × 0.9 mm. Whole-brain magnetic resonance spectroscopic imaging (MRSI) data were acquired using a 3D echo-planar spectroscopic imaging sequence[40]: TR = 1550 msec; TE = 17.6 msec; lipid inversion nulling with inversion time (TI) = 198 msec; spin-echo excitation with selection of a 135 mm axial slab covering the cerebrum; flip angle = 71°; FOV = 280 × 280 × 180 mm; matrix = 50 × 50 × 18; GRAPPA factor = 1.3; TA = 18 min; voxel resolution = 5.6 × 5.6 × 10 mm.

A two-dimensional ASL scan was acquired using a Proximal Inversion with Control of Off-Resonance Effects labeling scheme: TR = 2500 msec; TE = 16.18 msec; TI = 1800 msec; 12 slices; FOV = 256 × 256 mm; matrix = 64 × 64 mm; TA = 5 min; voxel resolution = 4 × 4 × 8 mm. Sixty pairs of axial label/control images were collected. All image acquisition parameters have been described in a previous study in participants with myalgic encephalomyelitis/chronic fatigue syndrome.[41]

Image processing

MRSI data were processed using the fully automated MRSI processing pipeline within the Metabolite Imaging and Data Analysis System software package.[42] Images were reconstructed, corrected for B0 shifts, interpolated to 64 × 64 × 32 points, and smoothed to achieve an effective voxel volume of 1.5 mL. The FITT2 module was used to carry out parametric spectral fitting and then normalized to institutional units using a tissue water reference,[42] which was acquired using an interleaved nonwater suppressed acquisition. Maps of the tissue distribution that corresponded to the spectroscopic image resolution spatial response function were obtained following segmentation of the T1-weighted MRI using Functional MRI of the Brain Group (FMRIB) Software Library/FMRIB Automated Segmentation Tool (FSL/FAST).[43] Metabolite ratio and tissue distribution images were nonlinearly transformed to 2 mm standard space. Gray and white matter segmentations were used as ROIs to investigate global gray and white matter abnormalities. A lobar atlas and modified version of Automated Anatomical Labeling (AAL) atlas were used as spatial reference[44]; smaller ROIs were combined to delineate 47 anatomical structures suitable for lower resolution MRSI data.

A modified version of the Johns Hopkins University (JHU) white matter tract atlas[45] was also used to delineate major white matter structures that have shown to be affected following TBI, that is, the internal capsule, anterior and posterior corona radiata, cingulum, sagittal striatum, superior longitudinal fasciculus, external capsule, and genu, body, and splenium of the corpus callosum.[46–48]

Data analysis

Metabolite data were corrected using the Project Review and Analysis module within Metabolite Imaging and Data Analysis System. Voxels were excluded from analysis if they had (1) fitted metabolite linewidth >13 Hz, (2) an outlying value >2.5 times the SD of all valid voxels over the image, and (3) a Cram r-Rao Lower Bounds for fitting of CR of >20%, (4) <80% gray or white matter, or (5) >30% cerebrospinal fluid contribution to the voxel volume. The inverse spatial transform generated during registration to Montreal

Neurological Institute (MNI) space was applied to the data to obtain atlas-defined ROIs in subject space. Spectra in each ROI were averaged in the Map Integrated Spectrum (MINT) module to obtain a single average spectrum, and spectral fitting was performed. Average spectra have higher signal-to-noise ratio and enable more accurate fitting; resultant maps for NAA, CR, CHO, and MI were extracted and ratios over CR were calculated.

Linear regression was also carried out in the Project Review and Analysis (PRANA) module to calculate the mean value of each metabolite ratio separately for gray and white matter in each brain lobe.

ASL data were processed using the standard processing pipeline within ASLtbx[49] for SPM12 within MATLAB. Data were visually assessed for accurate co-registration, contrast in anatomical structures, and artifacts including signal hyper-/hypo-intensities, distortions, and motion. Data were then smoothed with a 6-mm Gaussian kernel and each label/control pair was subtracted for quantification of cerebral blood flow (CBF) in mL/100 g/min. Mean CBF maps were linearly registered to the magnetization prepared rapid gradient echo image, then nonlinearly warped to 2-mm MNI space using FSL FMRIB Nonlinear Image Registration Tool (FNIRT).[50] Mean CBF was quantified in each ROI from the modified AAL atlas.

Statistics

Main analyses were conducted in SPSS Statistics v25. Univariate independent-samples *t*-tests were used to compare mean metabolite ratios between the TBI and control groups in each ROI. Homogeneity of variance of the distribution of outcome variables (metabolite ratios) across groups was tested using Levene's test, and nonparametric tests were used for outcomes that failed to meet the assumption. Adjusted degrees of freedom for those tests are indicated in Table 2. The dependent variables were (1) CHO/CR, (2) myo-inositol/creatine (MI/CR), and (3) NAA/CR in each ROI. Significance of group differences was assumed at $P < .05$ (uncorrected). We also used an additional false discovery rate of 0.01 to examine whether any results would reach significance at this threshold (equivalent to uncorrected $P < .002$). Equivalent independent-samples *t*-tests were used to compare mean CBF values between patients and controls in each ROI from the AAL atlas.

To investigate whether there was a relationship between metabolite ratios and pain, fatigue, anxiety, and depression in participants with TBI, regions with metabolite ratios that were significantly different between groups were then tested (two-tailed) for associations with severity of clinical symptoms using Spearman's rho (rs) and a significance threshold of $P < .05$.

RESULTS

Data from four participants in the TBI group were excluded owing to poor data quality and one participant did not complete the protocol, leaving data from 11 participants. None of the participants had had multiple injuries or history of previous/other TBI. The modes of injury for the sample were five motor vehicle crashes as occupants, four falls, one pedestrian struck by a motor vehicle, and one sports injury. For ethical reasons, participants were not asked

to stop taking medication. The proportion of participants on different classes of medication were as follows: antidepressants (4/11), anti-hypertensives (3/11), muscle relaxants (2/11), benzodiazepines (2/11), nonsteroidal anti-inflammatory drugs (2/11), anticonvulsants (2/11), and gabapentin (2/11).

Data from two control participants were excluded owing to visible movement during acquisition and an anatomical abnormality, leaving data from 10 control participants. Group means and results from between-groups *t*-tests comparing the questionnaire data are displayed in Table 1. Overall, the groups did not differ significantly in age. As expected, patients with TBI reported higher pain and fatigue severity, as well as higher anxiety and depression than controls.

All available voxels meeting data quality thresholds were used to calculate participants' mean ROI-based metabolite ratios.

There were no differences in metabolite ratios within whole-brain gray and white matter ROIs (Table 2). There was a statistical trend for higher MI/CR in the gray matter of participants with TBI ($P = .066$).

Global linear regression showed metabolite abnormalities in several brain lobes. Compared to controls, patients with TBI showed higher NAA/CR in the gray matter of the left parietal lobe (TBI: 1.149, controls: 0.924, $t[1, 19] = 2.393$, $P = .027$) and lower NAA/CR in the white matter of the left occipital lobe (TBI: 1.37, controls: 1.487, $t[1, 19]=2.348$, $P = .030$. However, these results did not survive correction for multiple comparisons. There was also a statistical trend of higher MI/CR in the gray matter of the left occipital lobe (TBI: 0.630, controls: 0.623, $t[1, 19] = 1.941$, $P = .067$). See Table 1 in Supporting Information for full results.

Figure 1 shows examples of spectra in the white and gray matter of the bilateral parietal lobes in a representative TBI participant and healthy control. Spectra are averaged over all voxels meeting quality thresholds within the ROI.

The mean percentage of available voxels in an ROI that met quality criteria ranged from 36.72% in the L frontal gyrus to 92.69% in the R Rolandic operculum (mean across all ROIs: 66.89% accepted voxels). Missing data on a person level occurred in three ROIs from control group members (R pallidum, L sagittal striatum, L anterior cingulate) where none of the available voxels within the ROIs met data quality thresholds. The range of mean number of accepted voxels per ROI was 8 (pallidum) to 730 (cerebellum). The *t*-tests were run with data from the remaining available participants, with reduced group sizes indicated in Table 3 where applicable.

Metabolic differences were observed in several brain regions (Table 3). CHO/CR and MI/CR were higher in participants with TBI compared to controls (Figures 2 and 3). Participants with TBI also showed significantly lower NAA/CR in two ROIs. None of the results survived corrections for multiple comparisons.

CBF data from two control participants were excluded owing to excessive subject motion during acquisition. Independent-samples *t*-tests in the remaining sample determined that regional CBF was not different between patients and controls in any AAL atlas ROIs (all $P > .05$; Table 4; Figure 4). Pulsed ASL does not yield reliable CBF quantification in white matter, so between-group differences were not assessed in the white matter ROIs.

Of the regions showing metabolic differences, seven also showed significant associations between metabolite ratios and self-reported symptoms, that is, pain, fatigue, depression, and anxiety (Table 5). Four of the seven regions were from the Johns Hopkins Universisty (JHU) atlas. Higher MI/CR was associated with higher levels of pain interference in the right posterior cingulate and right hippocampus, greater fatigue severity in the right sagittal stratum, right posterior cingulate, body of the corpus callosum, and left anterior limb of the internal capsule, and higher levels of depression in the right putamen and right posterior cingulate. Higher CHO/CR in the splenium of the corpus callosum and right posterior cingulate was associated with higher levels of anxiety.

Figure 5 shows the relationship between metabolite ratios in the right posterior cingulate and clinical symptoms in the patients with TBI.

Because of very low symptomatology in the healthy control group, who reported near-zero levels of pain, fatigue, anxiety, and depressive symptoms (see Table 1), correlations between self-reported symptoms and metabolite ratios could not be obtained.

DISCUSSION

The primary aim of the current study was to assess neurometabolic abnormalities across the brain in individuals in the chronic stage of a moderate or severe TBI. Males who had sustained a TBI at least 12 months before participating in the study underwent whole-brain MRS. Globally, participants in the chronic stages of TBI showed no neurometabolic abnormalities in gray or white matter compared to control participants without a history of TBI. Participants with TBI showed a trend for higher MI/CR in the gray matter.

Global linear regression to compare metabolites for gray and white matter in each brain lobe showed metabolite abnormalities in several brain lobes; however, these did not survive correction for multiple comparison. Compared to controls, patients with TBI showed lower NAA/CR in the white matter of the left occipital lobe but higher NAA/CR in the gray matter of the left parietal lobe. There was also a statistical trend of higher MI/CR in the gray matter of the left occipital lobe.

There are no whole-brain MRS studies that have investigated MI/CR in the chronic stage of TBI. Longitudinal studies have shown that reduced NAA in white matter persists during chronic stages of TBI studies.[31–33] One study in which patients with TBI showed higher NAA than controls at the chronic time point attributed the recovery and overshoot to ongoing cellular proliferation and membrane repair.[32] The absence of abnormalities relating to CHO/CR in the chronic stages is consistent with results from a study of pediatric patients with moderate/severe TBI[32] but contrary to another longitudinal study of whole-brain MRS[31]; however, it is important to note that the latter was a single-participant study and

used z-score image analysis rather than linear regression. It has been suggested that low CHO/CR at chronic time points may indicate cell death or lack of healthy turnover and repair.[32] However, with the small sample size and low statistical power of this study, we caution against the overinterpretation of our results until they are confirmed using larger sample sizes.

ROI analysis did reveal some metabolite abnormalities in several brain regions in patients with TBI and we demonstrated that the metabolite differences in the gray matter regions were not accompanied by abnormalities in blood supply. However, none of the findings survived correction for multiple comparison and, for that reason, they may be considered possible avenues for future research in this area. We observed widespread MI/CR elevations in patients with TBI, which affected cortical and subcortical regions in both hemispheres. MI is an important component of membrane phospholipids and cell culture studies have shown that the concentration of MI is higher in astrocytes than neurons.[16] Studies in humans and animal models have supported a link between MI and glial activation[51–54]; therefore, the MI/CR elevations seen in this study may indicate changes in glial density or activation, consistent with ongoing gliosis. There was an overlap of MI abnormalities and increases in CHO in the right posterior cingulate and the splenium of the corpus callosum, indicating abnormalities in cell membrane metabolism in addition to glial activation.

Both regions also showed extensive correlations with clinical symptom measures. CHO/CR ratios in the splenium of the corpus callosum positively correlated with HADS anxiety scores. The corpus callosum has previously been implicated in chronic TBI, whereby loss of white matter integrity (measured by diffusion tensor imaging) correlated with the severity of cognitive deficits.[55] The current study suggests that there may be prolonged proliferation and repair processes in the form of membrane synthesis/turnover or gliosis may be involved in the ongoing deterioration of the corpus callosum in chronic TBI and may relate to unresolving symptomatology.

The right posterior cingulate showed the most extensive associations with clinical symptoms. MI/CR elevations in this region were associated with higher pain, fatigue, and depressive symptoms, and CHO/CR elevations were associated with higher anxiety, suggesting that metabolite abnormalities in the posterior cingulate may be related to a variety of clinical symptoms in chronic TBI. The posterior cingulate, along with the medial prefrontal cortex and angular gyrus, is part of the default-mode network, responsible for sustaining attention and awareness. Previous studies have identified abnormalities in structural and functional connectivity within the default network, including the posterior cingulate, in patients in the chronic phase of TBI.[56] Such abnormalities are most often associated with impairments in sustained attention,[57] which was not assessed in the current study. However, our results suggest there may be a link between posterior cingulate abnormalities and ongoing clinical symptoms following a TBI.

MI elevations overlapped with decreases in NAA in the right putamen and were positively correlated with depressive symptom severity, suggesting that this region mediates some of the long-term symptoms experienced following TBI. NAA is a marker of neuronal integrity, with lower levels indicating neuronal injury. Together, MI and NAA abnormalities may

indicate ongoing gliosis. Given that the putamen is primarily involved in motor control, the connection between metabolite abnormalities in this region and depressive symptoms is not very clear; however, this region is emerging as a target for future study in patients with TBI.

Limitations

There are caveats to consider when interpreting our findings. First, metabolites were expressed as ratios over CR. CR is a marker of energy metabolism and its levels in the brain are assumed to be relatively stable. This method follows MRS conventions and allows for direct comparisons with other studies; however, any existing CR abnormalities in TBI patients could have affected the metabolite results. To avoid the confounding effects of CR, absolute metabolite concentrations can be quantified from MRS data; however, true absolute quantification (accounting for B0 and B1 inhomogeneity, T1 and T2 relaxation effects) has specific technical difficulties that limit its use in clinical research.

Second, our sample size was small compared to the number of comparisons conducted, so we determined statistical significance using uncorrected *P* values. None of the observed differences met the threshold for significance when false discovery rate corrections were applied.

Third, because this was a prospective study that recruited only males, we acknowledge that the findings lack generalizability and are pertinent only to men.

Fourth, the spatial resolution of the MRSI technique is relatively poor; therefore, significant partial volume effects with surrounding tissue will be present. However, these results and results from previous studies demonstrate that metabolic changes following a TBI are widespread so strong localized changes across the patient group were not anticipated.

Fifth, because the pulsed ASL technique does not yield reliable regional CBF measurements in white matter, we did not test whether metabolite group differences in these regions could have been due to abnormal blood supply. It is possible that moderate-to-severe TBIs result in reduced blood flow to the white matter, for example if arterial damage is sustained during the injury or secondary to subsequent pathophysiological processes. In this case, anoxia could be the primary source of metabolite abnormalities.

Lastly, though the majority of participants showed radiological abnormalities at the time of injury, the structural scans were not read by a neuroradiologist. The main objective of the study was to use MRS to detect abnormalities not visible on a T1-weighted image; however, future studies could incorporate this in order to characterize the extent of overlap of abnormalities between MRS and T1 images. Furthermore, we did not account for the presence of structural brain damage in our sample with scans to assess white matter lesions or atrophy. There was also heterogeneity with respect to modes and location of injury. This could have affected the ROI analyses and metabolite results; therefore, future research with larger samples could account for this more stringently and include multimodal structural studies, additional clinical outcomes, and other functional measures.

CONCLUSIONS

This study is one of few that has investigated neurometabolic abnormalities across the entire brain in a group of patients who had experienced a TBI more than 12 months before. Though we did not observe any statistically significant metabolite abnormalities in whole-brain or ROI analyses, we identified possible avenues for future investigation. It will be important to confirm whether there are widespread metabolite abnormalities and their relationship with clinical symptoms. Our findings support the hypothesis that prolonged proliferation and repair processes may persist in chronic stages of moderate-to-severe TBIs and may be related to the persistence of symptoms beyond expected recovery periods. Although these findings are preliminary, they are consistent with previous reports and suggest that sustaining a moderate-to-severe TBI may make an individual vulnerable to long-term pathophysiological changes in the brain that can be symptomatic.

Supplementary Material

Refer to Web version on PubMed Central for supplementary material.

ACKNOWLEDGMENTS

The authors wish to thank the TBI Model Systems for their assistance in recruitment, and Dr. Thomas Novack for reviewing the manuscript. This study was supported by the University of Alabama at Birmingham (Functional Neurorecovery Collaborative Pilot Grant) under Younger and National Institutes of Health-National Institute of Biomedical Imaging and Bioengineering (R01EB016064) under Maudsley. Dr. Younger was supported on this project by NIH-NINDS grant R01NS109529.

REFERENCES

1. Centers for Disease Control and Prevention. Report to Congress on Traumatic Brain Injury in the United States: Epidemiology and Rehabilitation. Atlanta, GA: Centers for Disease Control and Prevention; 2014.
2. Zaloshnja E, Miller T, Langlois JA, Selassie AW. Prevalence of long-term disability from traumatic brain injury in the civilian population of the United States, 2005. J Head Trauma Rehabil. 2008;23(6):394–400. [PubMed: 19033832]
3. Selassie AW, Zaloshnja E, Langlois JA, Miller T, Jones P, Steiner C. Incidence of long-term disability following traumatic brain injury hospitalization, United States, 2003. J Head Trauma Rehabil. 2008;23(2):123–131. [PubMed: 18362766]
4. Thurman DJ, Alverson C, Dunn KA, Guerrero J, Sniezek JE. Traumatic brain injury in the United States: a public health perspective. J Head Trauma Rehabil. 1999;14(6):602–615. [PubMed: 10671706]
5. Zanier ER, Fumagalli S, Perego C, Pischiutta F, de Simoni MG. Shape descriptors of the “never resting” microglia in three different acute brain injury models in mice. Intensive Care Med Exp. 2015;3(1):39. [PubMed: 26215806]
6. Loane DJ, Kumar A, Stoica BA, Cabatbat R, Faden AI. Progressive neurodegeneration after experimental brain trauma: association with chronic microglial activation. J Neuropathol Exp Neurol. 2014;73(1):14–29. [PubMed: 24335533]
7. Johnson VE, Stewart JE, Begbie FD, Trojanowski JQ, Smith DH, Stewart W. Inflammation and white matter degeneration persist for years after a single traumatic brain injury. Brain. 2013;136(Pt 1):28–42. [PubMed: 23365092]
8. Lozano D, Gonzales-Portillo GS, Acosta S, et al. Neuroinflammatory responses to traumatic brain injury: etiology, clinical consequences, and therapeutic opportunities. Neuropsychiatr Dis Treat. 2015;11:97–106. [PubMed: 25657582]

9. Tajiri N, Acosta SA, Shahaduzzaman M, et al. Intravenous transplants of human adipose-derived stem cell protect the brain from traumatic brain injury-induced neurodegeneration and motor and cognitive impairments: cell graft biodistribution and soluble factors in young and aged rats. J Neurosci. 2014;34(1):313–326. [PubMed: 24381292]
10. Acosta SA, Tajiri N, Shinozuka K, et al. Combination therapy of human umbilical cord blood cells and granulocyte colony stimulating factor reduces histopathological and motor impairments in an experimental model of chronic traumatic brain injury. PLoS One. 2014;9(3):e90953. [PubMed: 24621603]
11. Hernandez-Ontiveros DG, Tajiri N, Acosta S, Giunta B, Tan J, Borlongan CV. Microglia activation as a biomarker for traumatic brain injury. Front Neurol. 2013;4:30. [PubMed: 23531681]
12. Niyonkuru C, Wagner AK, Ozawa H, Amin K, Goyal A, Fabio A. Group-based trajectory analysis applications for prognostic biomarker model development in severe TBI: a practical example. J Neurotrauma. 2013;30(11):938–945. [PubMed: 23421760]
13. Scherbel U, Raghupathi R, Nakamura M, et al. Differential acute and chronic responses of tumor necrosis factor-deficient mice to experimental brain injury. Proc Natl Acad Sci U S A. 1999;96(15):8721–8726. [PubMed: 10411942]
14. Haley AP, Knight-Scott J. Proton magnetic resonance spectroscopy (1H MRS): a practical guide for the clinical neuroscientist. Brain Imaging in Behavioral Medicine and Clinical Neuroscience. New York: Springer; 2011:83–91.
15. Brown M, Baradaran H, Christos PJ, Wright D, Gupta A, Tsiouris AJ. Magnetic resonance spectroscopy abnormalities in traumatic brain injury: a meta-analysis. J Neuroradiol. 2018;45(2):123–129. [PubMed: 28965789]
16. Brand A, Richter-Landsberg C, Leibfritz D. Multinuclear NMR studies on the energy metabolism of glial and neuronal cells. Dev Neurosci. 1993;15(3–5):289–298. [PubMed: 7805581]
17. Ashwal S, Holshouser B, Tong K, et al. Proton spectroscopy detected myoinositol in children with traumatic brain injury. Pediatr Res. 2004;56(4):630–638. [PubMed: 15295080]
18. Sheth C, Prescot AP, Legarreta M, Renshaw PF, McGlade E, Yurgelun-Todd D. Increased myoinositol in the anterior cingulate cortex of veterans with a history of traumatic brain injury: a proton magnetic resonance spectroscopy study. J Neurophysiol. 2020;123(5):1619–1629. [PubMed: 32186438]
19. Ng SY, Lee AYW. Traumatic brain injuries: pathophysiology and potential therapeutic targets. Front Cell Neurosci. 2019;13:528. [PubMed: 31827423]
20. Farkas O, Povlishock JT. Cellular and subcellular change evoked by diffuse traumatic brain injury: a complex web of change extending far beyond focal damage. Prog Brain Res. 2007;161:43–59. [PubMed: 17618969]
21. Govind V, Gold S, Kaliannan K, et al. Whole-brain proton MR spectroscopic imaging of mild-to-moderate traumatic brain injury and correlation with neuropsychological deficits. J Neurotrauma. 2010;27(3):483–496. [PubMed: 20201668]
22. Maudsley AA, Govind V, Levin B, Saigal G, Harris L, Sheriff S. Distributions of magnetic resonance diffusion and spectroscopy measures with traumatic brain injury. J Neurotrauma. 2015;32(14):1056–1063. [PubMed: 25333480]
23. Juengst SB, Kumar RG, Failla MD, Goyal A, Wagner AK. Acute inflammatory biomarker profiles predict depression risk following moderate to severe traumatic brain injury. J Head Trauma Rehabil. 2015;30(3):207–218. [PubMed: 24590155]
24. Zgaljardic DJ, Seale GS, Schaefer LA, Temple RO, Foreman J, Elliott TR. Psychiatric disease and post-acute traumatic brain injury. J Neurotrauma. 2015;32(23):1911–1925. [PubMed: 25629222]
25. Mollayeva T, Kendzerska T, Mollayeva S, Shapiro CM, Colantonio A, Cassidy JD. A systematic review of fatigue in patients with traumatic brain injury: the course, predictors and consequences. Neurosci Biobehav Rev. 2014;47:684–716. [PubMed: 25451201]
26. Cantor JB, Ashman T, Gordon W, et al. Fatigue after traumatic brain injury and its impact on participation and quality of life. J Head Trauma Rehabil. 2008;23(1):41–51. [PubMed: 18219234]
27. Bushnik T, Englander J, Wright J. Patterns of fatigue and its correlates over the first 2 years after traumatic brain injury. J Head Trauma Rehabil. 2008;23(1):25–32. [PubMed: 18219232]

28. Widerstrom-Noga E, Govind V, Adcock JP, Levin BE, Maudsley AA. Subacute pain after traumatic brain injury is associated with lower insular N-acetylaspartate concentrations. J Neurotrauma. 2016;33(14):1380–1389. [PubMed: 26486760]
29. Defrin R, Gruener H, Schreiber S, Pick CG. Quantitative somatosensory testing of subjects with chronic post-traumatic headache: implications on its mechanisms. Eur J Pain. 2010;14(9):924–931. [PubMed: 20363652]
30. Ofek H, Defrin R. The characteristics of chronic central pain after traumatic brain injury. Pain. 2007;131(3):330–340. [PubMed: 17689190]
31. Maudsley AA, Govind V, Saigal G, Gold SG, Harris L, Sheriff S. Longitudinal MR spectroscopy shows altered metabolism in traumatic brain injury. J Neuroimaging. 2017;27(6):562–569. [PubMed: 28736910]
32. Babikian T, Alger JR, Ellis-Blied MU, et al. Whole brain magnetic resonance spectroscopic determinants of functional outcomes in pediatric moderate/severe traumatic brain injury. J Neurotrauma. 2018;35(14):1637–1645. [PubMed: 29649959]
33. Holshouser B, Pivonka-Jones J, Nichols JG, et al. Longitudinal metabolite changes after traumatic brain injury: a prospective pediatric magnetic resonance spectroscopic imaging study. J Neurotrauma. 2019;36(8):1352–1360. [PubMed: 30351247]
34. Maudsley AA, Goryawala MZ, Sheriff S. Effects of tissue susceptibility on brain temperature mapping. Neuroimage. 2017;146:1093–1101. [PubMed: 27693198]
35. Frost RB, Farrer TJ, Primosch M, Hedges DW. Prevalence of traumatic brain injury in the general adult population: a meta-analysis. Neuroepidemiology. 2013;40(3):154–159. [PubMed: 23257914]
36. Munivenkatappa A, Agrawal A, Shukla DP, Kumaraswamy D, Devi BI. Traumatic brain injury: does gender influence outcomes? Int J Crit Illn Inj Sci. 2016;6(2):70–73. [PubMed: 27308254]
37. Cleeland CS, Ryan KM. Pain assessment: global use of the brief pain inventory. Ann Acad Med Singapore. 1994;23(2):129–138. [PubMed: 8080219]
38. Krupp LB, LaRocca NG, Muir-Nash J, Steinberg AD. The fatigue severity scale. Application to patients with multiple sclerosis and systemic lupus erythematosus. Arch Neurol. 1989;46(10):1121–1123. [PubMed: 2803071]
39. Zigmond AS, Snaith RP. The hospital anxiety and depression scale. Acta Psychiatr Scand. 1983;67(6):361–370. [PubMed: 6880820]
40. Ebel A, Maudsley AA. Improved spectral quality for 3D MR spectroscopic imaging using a high spatial resolution acquisition strategy. Magn Reson Imaging. 2003;21(2):113–120. [PubMed: 12670597]
41. Mueller C, Lin JC, Sheriff S, Maudsley AA, Younger JW. Evidence of widespread metabolite abnormalities in Myalgic encephalomyelitis/chronic fatigue syndrome: assessment with whole-brain magnetic resonance spectroscopy. Brain Imaging Behav. 2019;14:562–572.
42. Maudsley AA, Domenig C, Govind V, et al. Mapping of brain metabolite distributions by volumetric proton MR spectroscopic imaging (MRSI). Magn Reson Med. 2009;61(3):548–559. [PubMed: 19111009]
43. Zhang Y, Brady M, Smith S. Segmentation of brain MR images through a hidden Markov random field model and the expectation-maximization algorithm. IEEE Trans Med Imaging. 2001;20(1):45–57. [PubMed: 11293691]
44. Tzourio-Mazoyer N, Landeau B, Papathanassiou D, et al. Automated anatomical labeling of activations in SPM using a macroscopic anatomical parcellation of the MNI MRI single-subject brain. Neuroimage. 2002;15(1):273–289. [PubMed: 11771995]
45. Mori S, Oishi K, Faria AV. White matter atlases based on diffusion tensor imaging. Curr Opin Neurol. 2009;22(4):362–369. [PubMed: 19571751]
46. Aoki Y, Inokuchi R, Gunshin M, Yahagi N, Suwa H. Diffusion tensor imaging studies of mild traumatic brain injury: a meta-analysis. J Neurol Neurosurg Psychiatry. 2012;83(9):870–876. [PubMed: 22797288]
47. Hulkower MB, Poliak DB, Rosenbaum SB, Zimmerman ME, Lipton ML. A decade of DTI in traumatic brain injury: 10 years and 100 articles later. AJNR Am J Neuroradiol. 2013;34(11):2064–2074. [PubMed: 23306011]

48. Shenton ME, Hamoda HM, Schneiderman JS, et al. A review of magnetic resonance imaging and diffusion tensor imaging findings in mild traumatic brain injury. Brain Imaging Behav. 2012;6(2):137–192. [PubMed: 22438191]

49. Wang Z, Aguirre GK, Rao H, et al. Empirical optimization of ASL data analysis using an ASL data processing toolbox: ASLtbx. Magn Reson Imaging. 2008;26(2):261–269. [PubMed: 17826940]

50. Andersson JL, Jenkinson M, Smith S. Non-linear optimisation: FMRIB Technical Report TR07JA1. 2007.

51. Bitsch A, Bruhn H, Vougioukas V, et al. Inflammatory CNS demyelination: histopathologic correlation with in vivo quantitative proton MR spectroscopy. AJNR Am J Neuroradiol. 1999;20(9):1619–1627. [PubMed: 10543631]

52. Rothermundt M, Ohrmann P, Abel S, et al. Glial cell activation in a subgroup of patients with schizophrenia indicated by increased S100B serum concentrations and elevated myo-inositol. Prog Neuropsychopharmacol Biol Psychiatry. 2007;31(2):361–364. [PubMed: 17081670]

53. Filibian M, Frasca A, Maggioni D, Micotti E, Vezzani A, Ravizza T. In vivo imaging of glia activation using 1H-magnetic resonance spectroscopy to detect putative biomarkers of tissue epileptogenicity. Epilepsia. 2012;53(11):1907–1916. [PubMed: 23030308]

54. Chen SQ, Wang PJ, Ten GJ, Zhan W, Li MH, Zang FC. Role of myo-inositol by magnetic resonance spectroscopy in early diagnosis of Alzheimer's disease in APP/PS1 transgenic mice. Dement Geriatr Cogn Disord. 2009;28(6):558–566. [PubMed: 20093832]

55. Arenth PM, Russell KC, Scanlon JM, Kessler LJ, Ricker JH. Corpus callosum integrity and neuropsychological performance after traumatic brain injury: a diffusion tensor imaging study. J Head Trauma Rehabil. 2014;29(2):E1–E10.

56. Sharp DJ, Beckmann CF, Greenwood R, et al. Default mode network functional and structural connectivity after traumatic brain injury. Brain. 2011;134(Pt 8):2233–2247. [PubMed: 21841202]

57. Bonnelle V, Leech R, Kinnunen KM, et al. Default mode network connectivity predicts sustained attention deficits after traumatic brain injury. J Neurosci. 2011;31(38):13442–13451. [PubMed: 21940437]

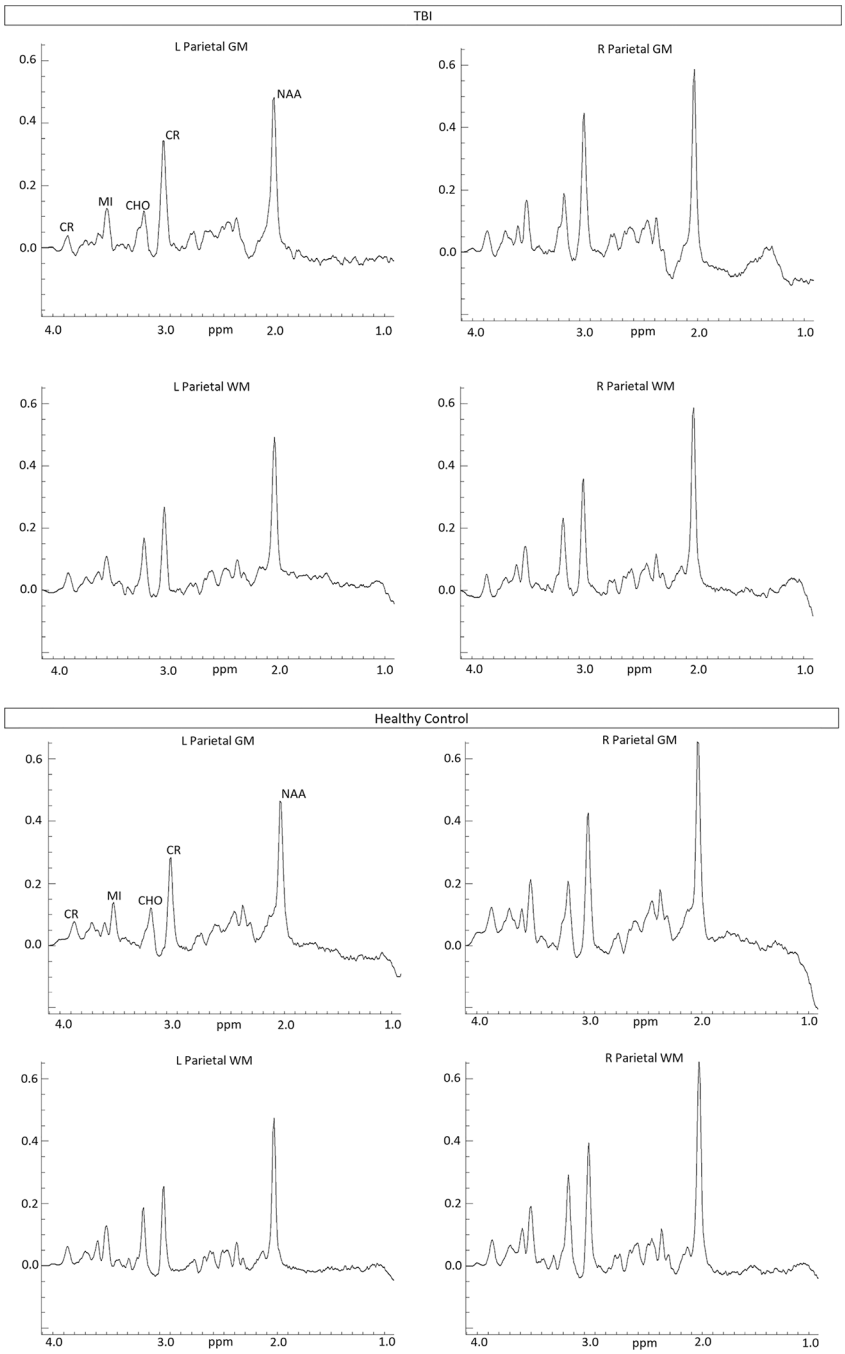

FIGURE 1.

Example average spectra from select regions of interest in a representative TBI patient and healthy control. Abbreviations: CHO, choline; CR, creatine; MI, myo-inositol; NAA, N-acetylaspartate; GM, gray matter; TBI, traumatic brain injury; WM, white matter

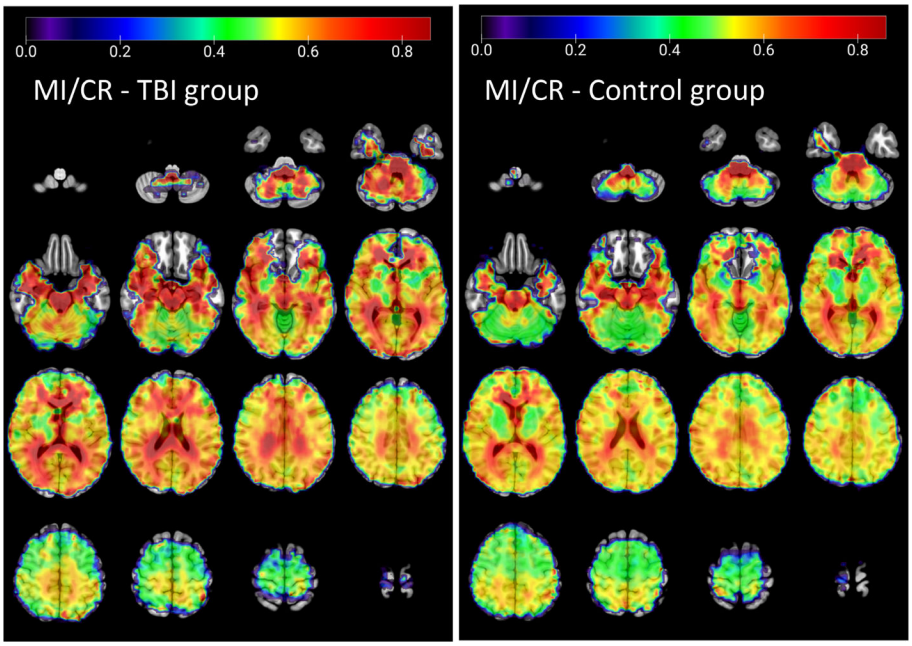

FIGURE 2.

Average MI/CR ratios in the TBI group (left) and control group (right). Metabolite maps are overlaid on an MNI standard brain for reference. Abbreviations: MI/CR, myo-inositol/creatine; MNI, Montreal Neurosciences Institute; TBI, traumatic brain injury

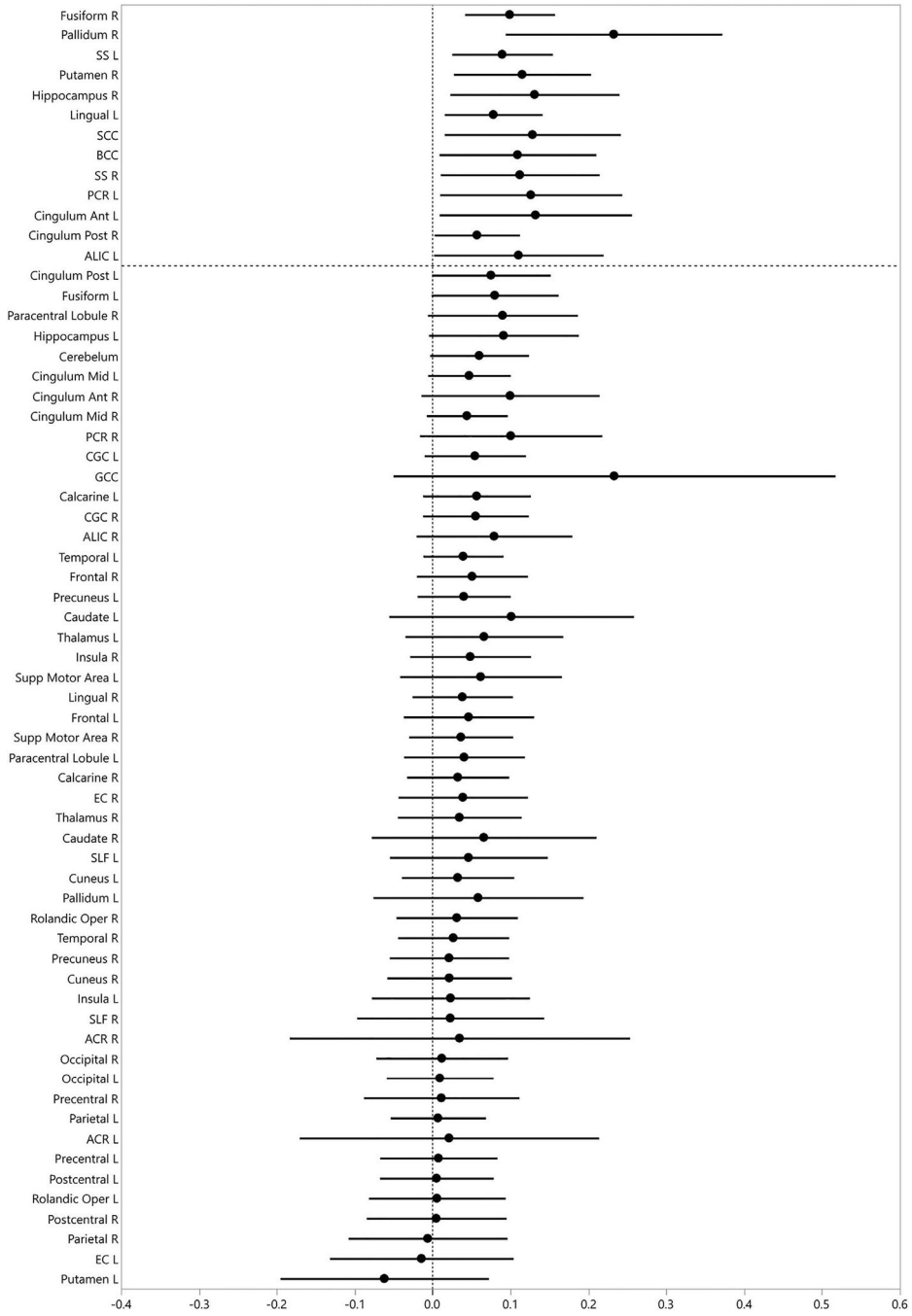

FIGURE 3.

The circle indicates the mean difference in MI/CR levels between patients with traumatic brain injury and controls. Error bars indicate 95% confidence intervals of the mean difference. Group differences that are significant are above the dotted line. Abbreviations: ACR, anterior corona radiata; ALIC, anterior limb of internal capsule; BCC, body of corpus callosum; CGC, cingulum (cinguate gyrus); EC, external capsule; GCC, genu of corpus callosum; MI/CR, myo-inositol/creatine; PCR, posterior corona radiata; SLF, superior longitudinal fasciculus; SS, sagittal stratum

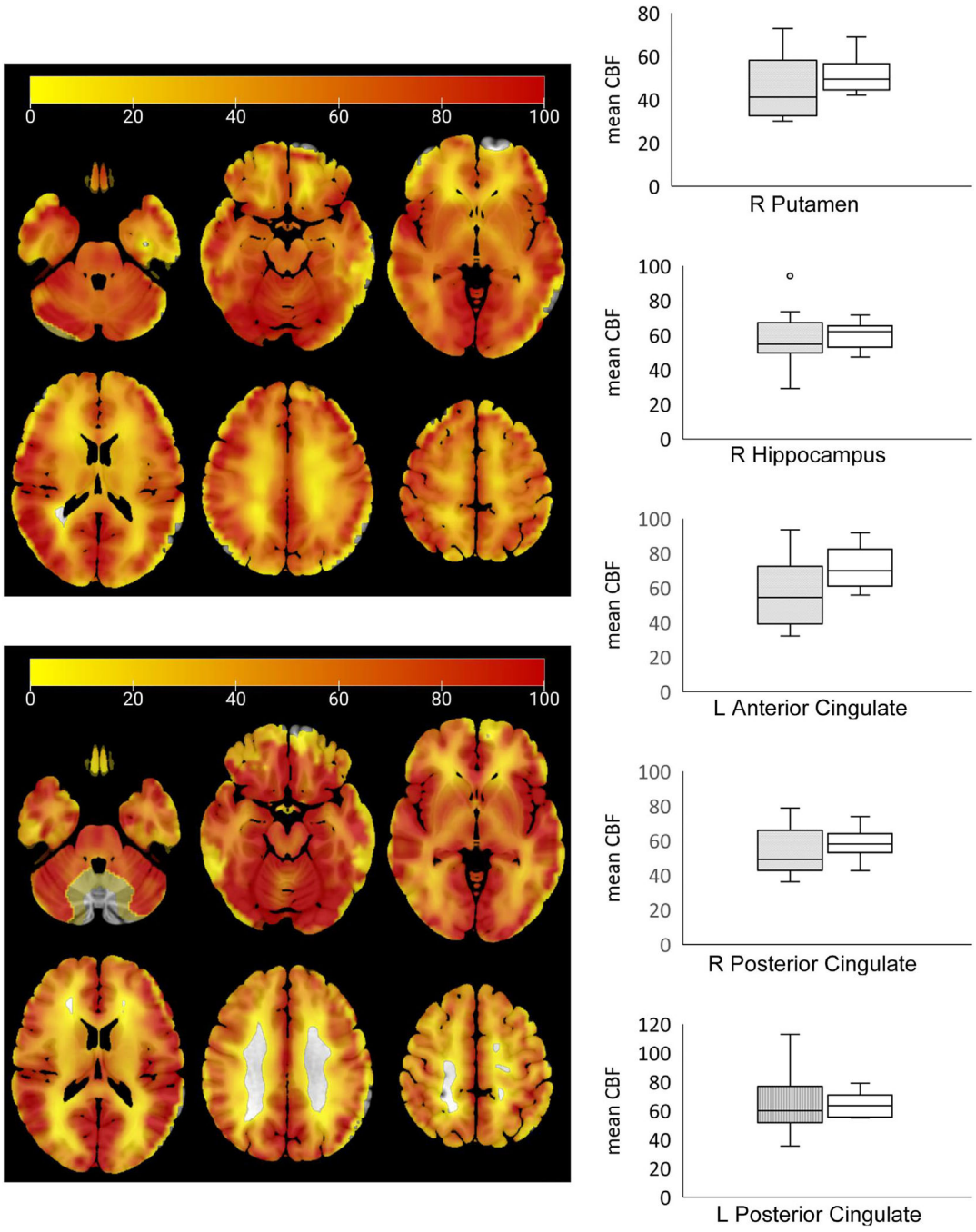

FIGURE 4.

Representative mean CBF maps in a patient with a TBI (top) and healthy control (bottom). Whisker plots show mean differences between the TBI group (gray fill) and healthy controls (no fill). Abbreviations: CBF, cerebral blood flow; TBI, traumatic brain injury

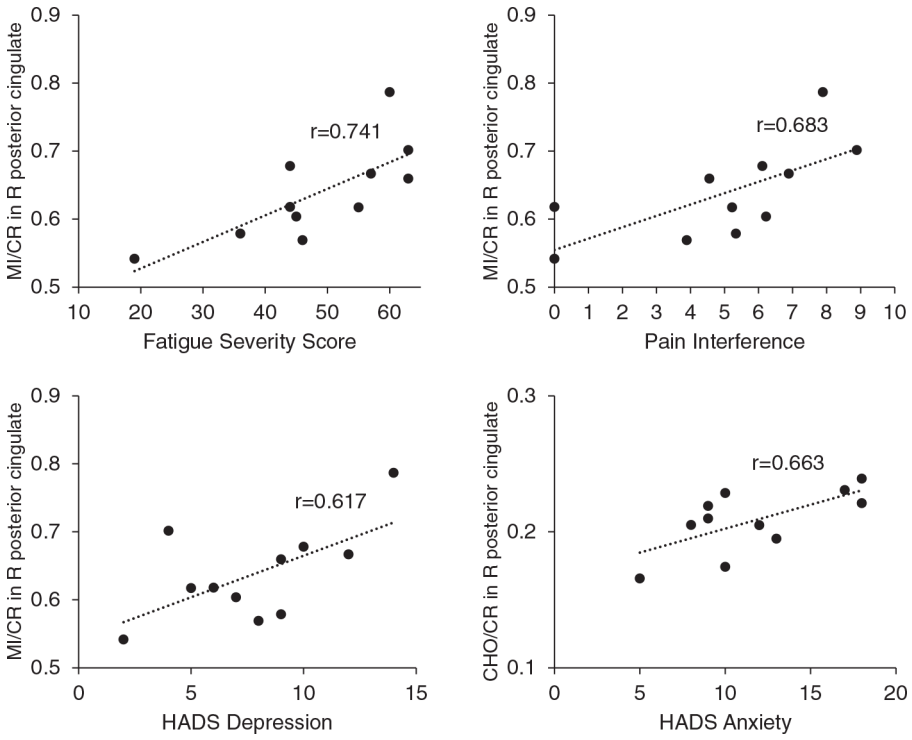

FIGURE 5.

Relationship between MI/CR ratios in the right posterior cingulate and clinical symptoms in the patients with traumatic brain injury. Abbreviations: CHO/CR, choline/creatine; HADS, Hospital Anxiety and Depression Scale; MI/CR, myo-inositol/creatine

TABLE 1

Group means and their standard deviations for questionnaire data at baseline

	TBI group (n = 11)		Control group (n = 10)		
	Mean	**SD**	**Mean**	**SD**	***P***
Age (years)	37.64	12.86	37.60	12.24	.995
Pain severity (0–10)	4.95	3.07	0.13	0.32	<.001
Pain interference (0–10)	5.00	2.85	0.22	0.07	.001
Fatigue severity (9–63)	48.36	13.24	10.80	2.57	<.001
Anxiety (0–21)	11.73	4.34	1.60	2.01	<.001
Depression (0–21)	7.82	3.52	0.20	0.42	<.001
Time since injury (months)	16.8	4.6	—	—	—
Moderate vs severe injury	6/5				

Note: P values are from independent-samples *t*-tests comparing the TBI and control group means.

Abbreviation: TBI, traumatic brain injury.

TABLE 2

Mean metabolite ratios and their standard deviations in the TBI and control groups in whole-brain gray and white matter

		TBI group	Controls				
Metabolite	**ROI**	**Mean (SD)**	**Mean (SD)**	**Mean difference 95% CI**	**t**	**df**	***P* value**
CHO/CR	Gray matter	0.197 (0.030)	0.192 (0.023)	0.004 (−0.020, 0.029)	0.380	19	.708
	White matter	0.261 (0.031)	0.252 (0.025)	0.009 (−0.017, 0.035)	0.724	19	.478
MI/CR	Gray matter	0.516 (0.082)	0.456 (0.056)	0.061 (−0.004, 0.126)	1.950	19	.066
	White matter	0.648 (0.123)	0.587 (0.062)	0.061 (−0.030, 0.151)	1.404	19	.177
NAA/CR	Gray matter	0.596 (0.141)	0.587 (0.106)	0.009 (−0.105, 0.124)	0.170	19	.867
	White matter	1.220 (0.110)	1.291 (0.095)	−0.072 (−0.166, 0.023)	−1.582	19	.130

Note: t-values and *P* values are from independent-samples *t*-tests comparing the metabolite ratio means.

Abbreviations: CHO/CR, choline/creatine; CI, confidence interval; MI/CR, myo-inositol/creatine; NAA/CR, N-acetylaspartate/creatine; ROI, region of interest; TBI, traumatic brain injury.

TABLE 3

Mean metabolite ratios and their standard deviations in the TBI and control groups in ROIs showing metabolic differences between groups

		TBI group		Controls					
Metabolite	**ROI**	**Mean (SD)**	**Number (%) voxels**	**Mean (SD)**	**Number (%) voxels**	**Mean difference 95% CI**	**t**	**df**	***P* value**
CHO/CR	R posterior cingulate	0.208 (0.023)	24 (91.87)	0.176 (0.023)	20 (82.06)	0.032 (0.011, 0.053)	3.192	19	.005
	Splenium of corpus callosum	0.290 (0.027)	85 (76.26)	0.668 (0.092)	84 (79.74)	0.032 (0.004, 0.061)	2.355	19	.029
	L posterior cingulate	0.226 (0.032)	15 (80.88)	0.193 (0.036)	14 (79.97)	0.032 (0.000, 0.064)	2.105	19	.050
MI/CR	R fusiform gyrus	0.659 (0.077)	84 (63.75)	0.560 (0.042)	72 (58.32)	0.099 (0.041, 0.156)	3.585	19	.002
	R pallidum	0.555 (0.165)	8 (50.98)	0.322 (0.101)	8 (50.42)	0.233 (0.093, 0.372)	3.528	17[b]	.003
	L sagittal striatum	0.703 (0.084)	21 (67.94)	0.613 (0.049)	21 (77.23)	0.089 (0.025, 0.154)	2.904	18[c]	.009
	R putamen	0.514 (0.088)	31 (53.49)	0.399 (0.105)	35 (64.52)	0.115 (0.027, 0.203)	2.733	19	.013
	R hippocampus	0.804 (0.158)	32 (62.15)	0.673 (0.044)	30 (60.78)	0.131 (0.022, 0.239)	2.636	11.656[a]	.022
	L lingual gyrus	0.621 (0.077)	102 (79.58)	0.543 (0.058)	112 (88.51)	0.078 (0.152, 0.141)	2.600	19	.018
	Splenium of corpus callosum	0.796 (0.146)	85 (76.26)	0.668 (0.092)	84 (79.74)	0.128 (0.015, 0.241)	2.375	19	.028
	Body of corpus callosum	0.724 (0.147)	69 (71.86)	0.615 (0.039)	75 (83.22)	0.109 (0.008, 0.210)	2.370	11.516[a]	.036
	R sagittal striatum	0.802 (0.142)	22 (78.40)	0.690 (0.066)	20 (77.10)	0.112 (0.010, 0.214)	2.347	14.451[a]	.034
	L posterior corona radiata	0.729 (0.153)	18 (85.86)	0.603 (0.092)	19 (92.32)	0.126 (0.009, 0.243)	2.258	19	.036
	L anterior cingulate	0.754 (0.136)	20 (26.13)	0.622 (0.127)	27 (39.43)	0.132 (0.009, 0.256)	2.247	18[c]	.037
	R posterior cingulate	0.638 (0.070)	24 (91.87)	0.581 (0.047)	20 (82.06)	0.057 (0.002, 0.112)	2.175	19	.042
	L anterior limb of internal capsule	0.634 (0.149)	55 (74.06)	0.524 (0.078)	54 (77.39)	0.110 (0.001, 0.219)	2.153	15.372[a]	.048
NAA/CR	R putamen	0.948 (0.149)	31 (53.49)	1.081 (0.095)	35 (64.52)	−0.133 (−0.249, −0.018)	−2.416	19	.026
	R anterior limb of internal capsule	1.104 (0.181)	53 (72.44)	1.248 (0.090)	57 (82.61)	−0.144 (−0.276, −0.013)	−2.338	14.975[a]	.034

Note: T-values and *P* values are from independent-samples *t*-tests comparing the metabolite ratio means. TBI group, n = 11; control group, n = 10.

Abbreviations: CHO/CR, choline/creatine; CI, confidence interval; L, left; MI/CR, myo-inositol/creatine; NAA/CR, N-acetylaspartate/creatine; R, right; ROI, region of interest; TBI, traumatic brain injury.

[a]df adjusted for unequal variances.

[b]Missing data from two control participants.

[c]Missing data from one control participants.

TABLE 4

Mean CBF values (mL/100 g/min) and their standard deviations in gray matter ROIs that showed significant metabolic differences between groups

	TBI group	Controls			
ROI	**Mean (SD)**	**Mean (SD)**	**t**	**df**	***P* value**
R putamen	46.177 (14.912)	51.508 (8.754)	0.900	17	.380
R hippocampus	58.218 (16.743)	59.989 (7.918)	0.276	17	.786
L anterior cingulate	56.649 (18.847)	72.172 (12.373)	2.026	17	.059
R posterior cingulate	53.857 (13.708)	58.301 (9.246)	0.792	17	.439
L posterior cingulate	64.241 (20.441)	64.304 (8.606)	0.008	17	.994

Note: T-values and *P* values are from independent-samples *t*-tests comparing the CBF group means. TBI group: n = 11; control group: n = 8.

Abbreviations: CBF, cerebral blood flow; ROI, region of interest; TBI, traumatic brain injury.

TABLE 5

Significant correlations between metabolite ratios and self-reported symptoms in the TBI group in regions showing metabolic differences

Metabolite	ROI	r_s	*P*
Associations with pain interference			
MI/CR	R posterior cingulate	0.684	.020
	R hippocampus	0.676	.022
Associations with fatigue severity			
MI/CR	R sagittal stratum	0.789	.004
	R posterior cingulate	0.741	.009
	Body of corpus callosum	0.719	.013
	L anterior limb of internal capsule	0.673	.023
Associations with HADS anxiety			
CHO/CR	Splenium of corpus callosum	0.731	.011
	R posterior cingulate	0.663	.026
Associations with HADS depression			
MI/CR	R putamen	0.729	.011
	R posterior cingulate	0.617	.043

Abbreviations: CHO/CR, choline/creatine; HADS, Hospital Anxiety and Depression Scale; MI/CR, myo-inositol/creatine; ROI, region of interest; TBI, traumatic brain injury.